Forschungszentrum Karlsruhe
Technik und Umwelt

Wissenschaftliche Berichte
FZKA 6093

A Simple Model for the Elasticity of Granular Materials in Fusion Breeding Blankets

L. Bühler

Institut für Angewandte Thermo- und Fluiddynamik
Projekt Kernfusion

Mai 1998

Forschungszentrum Karlsruhe

Technik und Umwelt

Wissenschaftliche Berichte

FZKA 6093

A simple model for the elasticity of granular materials in fusion breeding blankets

L. Bühler

Institut für Angewandte Thermo- und Fluiddynamik
Projekt Kernfusion

Forschungszentrum Karlsruhe GmbH, Karlsruhe
1998

Als Manuskript gedruckt

Forschungszentrum Karlsruhe GmbH
Postfach 3640, 76021 Karlsruhe

Mitglied der Hermann von Helmholtz-Gemeinschaft
Deutscher Forschungszentren (HGF)

ISSN 0947-8620

A simple model for the elasticity of granular materials in fusion breeding blankets

Abstract

A simple model for elastic properties in packed beds of granular material is described. It is assumed that the packing is initially dense but with small gaps between some potential contact points. These gaps close during elastic loading and increase progressively the stiffness of the packing. The hysteresis during uniaxial compression cycles can be partly related to wall friction. Results are applied for Li_2SiO_4 pebbles and compared to some experimental data.

Ein einfaches Elastizitätsmodell für granulare Materialien in Fusionsblankets

Zusammenfassung

In diesem Bericht wird ein einfaches Modell zur Beschreibung des elastischen Verhaltens in Schüttbetten dargestellt. Es wird vorausgesetzt, daß die Schüttung in einer dichten Packung vorliegt, die jedoch kleine Lücken zwischen einigen potentiellen Kontaktstellen erlaubt. Während einer elastischen Kompression schließen sich diese Lücken und erhöhen zunehmend die Steifigkeit der Packung. Es wird ferner gezeigt, daß die Hysterese, die in einaxialen Kompressionsversuchen beobachtet wird, teilweise auf Wandreibungseffekte zurückzuführen ist. Ergebnisse werden für Li_2SiO_4 mit experimentellen Daten verglichen.

Contents

1 Introduction

A ceramic breeding blanket for fusion reactors is considered as one of the promising designs. The current design considered at the FZK as shown in figure 1 has been proposes e.g. by Dalle Donne, Fischer, Norajitra, Reimann and Reiser (1995). The blanket segment is split by horizontal plates into a number of subregions, alternatingly filled with the breeding ceramic material lithiumorthosilicate, Li_4SiO_4, and the neutron multiplier beryllium, Be (see figure 2). Both materials are used in the form of small spheres as compact assemblies of granular material. The walls separating Li_4SiO_4 from Be have internal cooling channels through which the fusion heat is removed by high-pressure helium flow. The breeding product tritium required as "plasma fuel" in the fusion process is removed from the packed beds by a low-pressure helium purge flow.

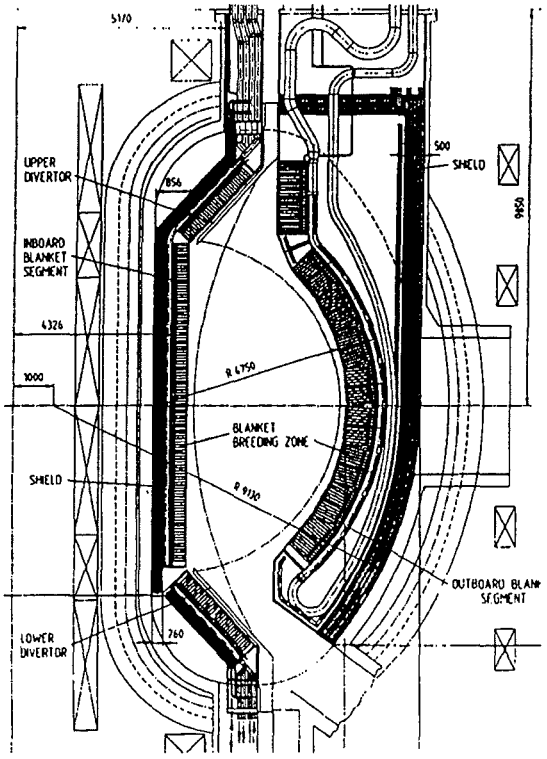

Figure 1: Sketch of the design for a ceramic fusion breeding blanket currently investigated at the Forschungszentrum Karlsruhe (Dalle Donne et al. (1995)).

Up to now there exist no accurate predictions or even reliable estimates (S. Malang, personal communication) for wall stresses caused by mechanical interaction between the pebble bed and the walls. The intention of the present report is to characterize the elastic behavior of a dense bed of granular particles of the breeding material. It will be assumed that the packing has initially the most dense arrangement. The particles will not be rearranged during compression. This assumption is justified if isotropic compression is considered. If the state of stress, however, is strongly anisotropic one has to take into account in addition macroscopic movements of the particles over distances much larger than the particles diameters. This and other problems like thermal stresses,

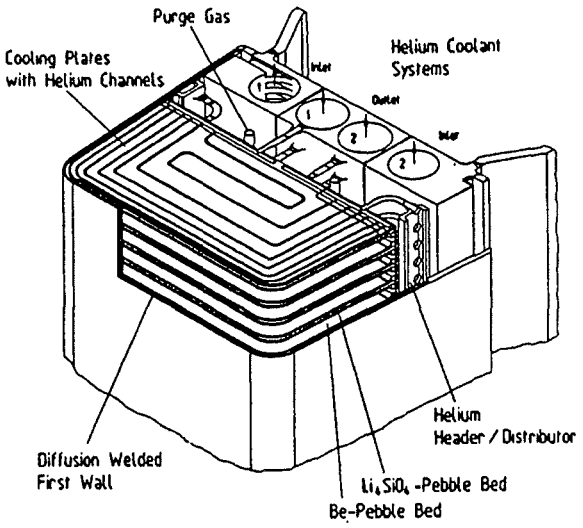

Figure 2: Poloidal portion of the outboard blanket (Dalle Donne et al. (1995)).

plastic deformation or creep are skipped and left for future research.

In this report an elastic model will be derived using ideas already published by Ko and Scott (1967). The results are compared with experimental data obtained by Reimann and Müller (1998) or with previous experimental date from the same group. A typical diagram of experimentally obtained Oedometer data is shown in the figure 3. This plot shows characteristic features observed in all experiments. During a first compression the bed behaves relatively weak. The reason may be the fact that not all particles have jet found their optimal position. If the stress is released the bed extends in volume. However, the particles which have found a better position will keep this so that the bed does not reach the initial volume. The second compression starts now with the better granular grid and behaves much stiffer than the first compression. There may be some reorganization of the bed even during several proceeding loading and relaxation cycles. After a number of cycles all particles have found their optimal position so that no further reorganization of granular contacts will occur. Several loading and unloading cycles fall practically on the same hysteresis curve. The hysteresis may be caused by wall or internal friction.

For the behavior of a DEMO blanket the most important part of the experimental curve is that of first compression since this curve may determine the maximal stresses in the bed and in the walls (J. Reimann & S. Malang, personal communication). Nevertheless, the present report focuses on the elastic behavior of the bed after it has reached the most dense packing, i.e. after a number of operation cycles. **All results which are derived below are not valid for the first compression.** They are, however, valid for granular beds after a number of loading cycles and may be used for estimations during periodic thermal cycling of the blanket.

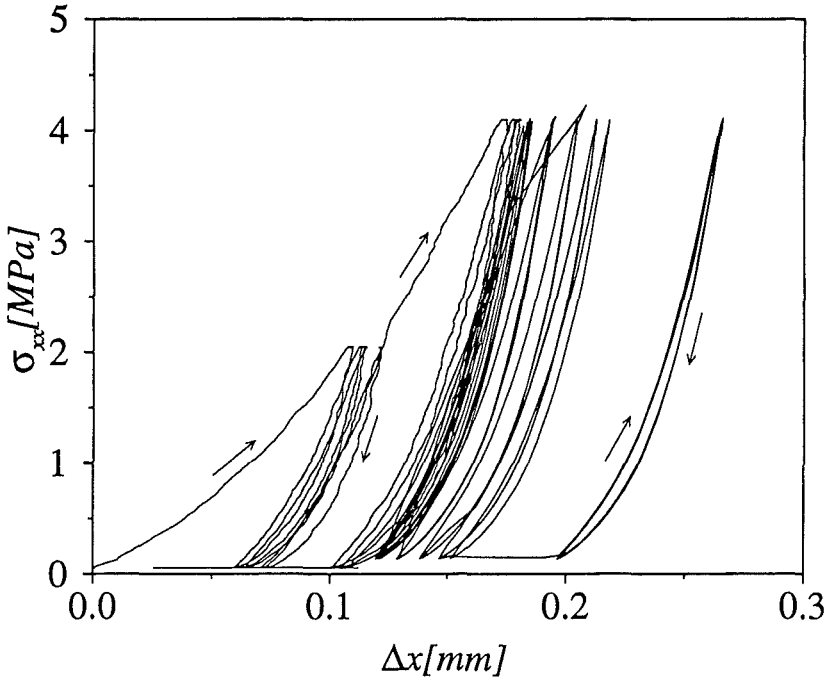

Figure 3: Typical data obtained experimentally (Reimann and Müller (1998))during cyclic uniaxial compression of Li_2SiO_4 at $400°C$. The pebbles had diameters between $0.25mm - 0.6mm$, the apparatus diameter was $60mm$ and the bed height was $14mm$. The first compression deviates considerably from proceeding ones since pebbles find better positions during compression. After a large number of cycles the bed finds its final density. Then, lines for compression and relaxation for different cycles become practically identical. The figure shows a number of cycles at the initial state and some at the end to which the experiment converges after several thousand cycles.

2 Elasticity

A material is called a *Cauchy elastic solid* if there exits a unique relation between the stress tensor $\boldsymbol{\sigma}$ and the deformation

$$\boldsymbol{\sigma} = \mathbf{f}(\mathbf{F}), \tag{1}$$

where $\mathbf{F}$ is the displacement gradient matrix (Hunter (1983), p148). In the isotropic case the most simple form of equation (1) is the linear version, known as Hook's law

$$\boldsymbol{\sigma} = \lambda(\nabla \cdot \mathbf{u})\mathbf{I} + 2\mu\mathbf{e}. \tag{2}$$

The vector $\mathbf{u}$ stands for the displacement and $\mathbf{e}$ is the matrix of the strain components which reads for the *small displacement gradient approximation* in spatial coordinates x_i:

$$e_{ij} = \frac{1}{2}\left(\frac{\partial u_i}{\partial x_j} + \frac{\partial u_j}{\partial x_i}\right). \tag{3}$$

The parameters λ, μ are the Lamé constants and μ is also known as the shear modulus. Introducing the dimensionless quantity *Poisson's ratio* ν the equation (2) can be rewritten as

$$\boldsymbol{\sigma} = 2\mu\left(\frac{\nu}{1-2\nu}I_e\mathbf{I} + \mathbf{e}\right). \tag{4}$$

Here, $I_e = e_{ii} = \Delta V/V$ is the first invariant of the strain tensor and corresponds the change of volume. Using *Young's elastic modulus* $E = 2\mu(1+\nu)$ the equation (4) can be solved for $\mathbf{e}$ (Hunter (1983), p369).

$$\begin{array}{l} e_{11} = \frac{1}{E}\left[\sigma_{11} - \nu(\sigma_{22} + \sigma_{33})\right] \\ e_{22} = \frac{1}{E}\left[\sigma_{22} - \nu(\sigma_{33} + \sigma_{11})\right] \\ e_{33} = \frac{1}{E}\left[\sigma_{33} - \nu(\sigma_{11} + \sigma_{22})\right] \\ e_{12} = \frac{\sigma_{12}}{2\mu}, \quad e_{23} = \frac{\sigma_{23}}{2\mu}, \quad e_{13} = \frac{\sigma_{13}}{2\mu} \end{array} \tag{5}$$

The relations for the diagonal elements can be summarized to give

$$e_{ij} = \frac{1}{E}\left[(1+\nu)\sigma_{ij} - \nu\sigma_{kk}\right] \tag{6}$$

For many purposes it is convenient to decompose the stress tensor into a deviatoric part $\mathbf{s}'$ and into a spherical part $\mathbf{s}'' = -p\mathbf{I}$ where $p = -\frac{1}{3}\sigma_{kk}$ is called the pressure (see e.g. Durelli, Phillips and Tsao (1958)) as

$$\boldsymbol{\sigma} = \mathbf{s}' - p\mathbf{I}. \tag{7}$$

The pressure is related to the first strain invariant as

$$p = -KI_e = -K\Delta V/V \tag{8}$$

where K is the ratio of hydrostatic pressure to the applied volume shrink. This property is known as the bulk modulus and can be expressed with the Lamé constants as

$$K = \lambda + \frac{2}{3}\mu \tag{9}$$

or using Young's modulus and Poisson's ratio as

$$K = \frac{1}{3}\frac{E}{1-2\nu}. \tag{10}$$

The bulk modulus describes the elasticity of a body if the deviatoric part of stress is small. For axisymmetric applications, $\sigma_{22} = \sigma_{33}$, the deviatoric part of the stress tensor can be expressed by the scalar quantity $q = \sigma_{11} - \sigma_{22}$ as

$$\mathbf{s}' = \frac{q}{3}\begin{bmatrix} 2 & 0 & 0 \\ 0 & -1 & 0 \\ 0 & 0 & -1 \end{bmatrix}. \tag{11}$$

The equations displayed above describe the elastic behavior of a solid body. The elasticity of a sample of granular particles in form of cylinders (2D models) or spheres (3D applications), however, deviates from that of a solid sample of the same material. If the solid sample has a linear relation between stress $\boldsymbol{\sigma}$ and strain $\mathbf{e}$ according to equation (4), this is not necessarily the case for granular assemblies and is not observed generally in experiments.

3 Elasticity of granular materials

The behavior of a volume of granular particles is quite different from that of a solid sample of same size and material. This is manifested e.g. in Young's elastic modulus which is much smaller than for solid samples and most essentially it is strongly load-dependent. If the granular bed is subjected to a isotropic compression brittle particles may fracture if their internal stresses exceed the critical value σ_F. Ductile particles may undergo permanent plastic deformations for loads beyond the material yield stress σ_Y. Especially at very high temperatures the particles may change their shape plastically due to creep on a long time scale (see e.g. Reimann, Müller and Lenartz (1997a) where plastic creep on moderate time scales and sintering has been observed). The present report does not address the latter effect and focuses only on the elastic properties of granular packed beds. It will be possible to derive from considerations of representative fractions of volume (on the dimensions of the particle size) macroscopic relations (for samples much larger than the particle diameters) between stress, strain and other parameters temperature.

Besides these effects the particles may be rearranged if the ratio of principal stresses exceeds a critical value. On the macroscopic point of view the material seems to flow. This movement is quite different from the material plasticity observed in solid samples or in granular samples as mentioned above and is called the granular plasticity. This point is skipped in the present work and left for future research.

3.1 Elasticity of loosely packed granular materials

In loosely packed beds there may exist vacancies in the lattice or inter-particle bonds may be missing in polydisperse packings as shown in figure 4. This has a strong influence on the structural rigidity of the bed and "the elastic modulus of randomly diluted lattices vanishes for a proportion of present bonds P approaching P_c as"

$$E \sim (P - P_c)\,\tau \tag{12}$$

where τ is called the elastic critical exponent (Guyon, Roux, Hansen, Bideau, Troadec and Crapo (1990)).

3.2 Elasticity of dense granular materials

For applications in fusion engineering it is envisaged to have a packing density as high as possible so that the relation displayed above will not hold. It is observed that in dense beds of cylinders the force F applied is related to the displacement ΔL like

$$\frac{F}{F_0} = \left(\frac{\Delta L}{L}\right)^m . \tag{13}$$

The exponent m may vary in the range of $2.7 < m < 3.5$ depending on the degree of disorder or on the distribution of cylinder size. In any case, m is larger than the value of $m_H = 3/2$ as expected for an individual Hertz contact (Guyon et al. (1990)). However, a value of m as observed in experiments can be obtained numerically on the basis of a

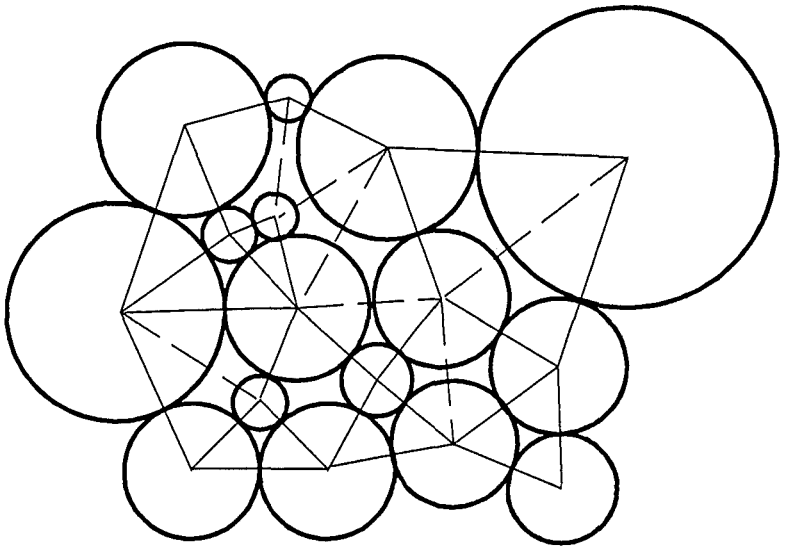

Figure 4: Polydisperse packing of discs: representative network. The full lines pass through the real contacts, the broken lines represent gaps (See Guyon et al. (1990), p381).

Hertzian theory of contact, if the radii of the cylinders are slightly fluctuating (Stauffer, Herrmann and Roux (1987)).

A 3D model on the basis of the Hertz theory for a granular medium formed by spheres has been used by Walton (1987). He describes the elastic behavior of a random packing of spheres, initially arranged as compact as possible. That means that the number of contacts does not change during compression. By this assumption that author derives formally, using statistical properties of the packing, a relation which gives the same behavior as the classical Hertz contact theory namely a variation of pressure p that correlates with the isotropic compression

$$\mathbf{e} = -\mathbf{I}\varepsilon \tag{14}$$

as $p \sim \varepsilon^{3/2}$. The elastic modulus is found to be proportional to $p^{1/3}$. Similar relations (same power laws) are obtained for the case of uniaxial compression (Oedometer tests). An interesting result of the cited paper is that the granular Poisson ratio ν^* of the whole assembly can be related to that of the particle's material, ν, by

$$\nu^* = \frac{\nu}{2\,(5 - 3\nu)} \tag{15}$$

for infinitely rough spheres while for smooth spheres

$$\nu^* = \frac{1}{4}, \tag{16}$$

completely independent of all parameters.

More recently Endres (1990) proposed a model that assumes a contact generation during compression. With such an assumption it is possible to obtain results that deviate

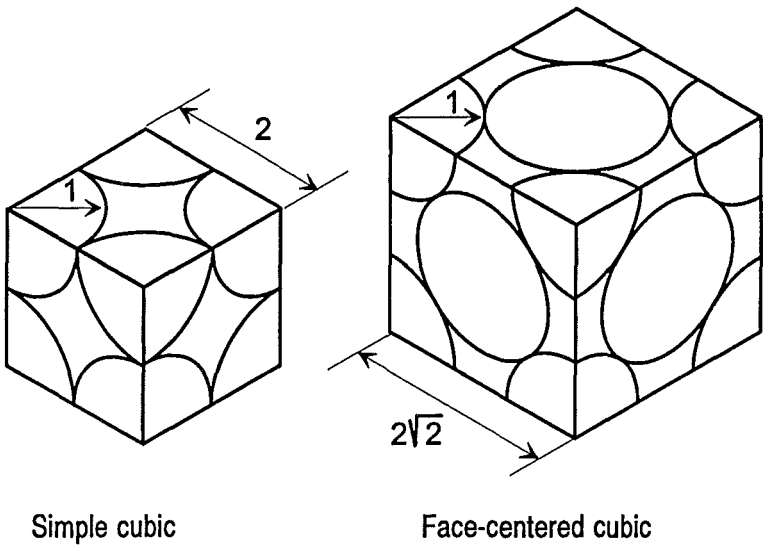

Figure 5: Unit elements of regular packings (see Ko and Scott (1967))

from the classical Hertz contact theory in the sense that the pressure increases faster than $\varepsilon^{3/2}$ or that the elastic modulus increases more rapidly than $p^{1/3}$. The analysis follows mainly the ideas of Walton (1987).

The idea of contact generation has been used much earlier by Ko and Scott (1967). These authors already proposed a model in which some spheres are initially in contact while between others potential contact points initial gaps are present. During increasing load gaps close successively and increase the stiffness of the packing much faster than the pure Hertz theory of contact would predict. At that time it was known that the Hertzian theory of contact does not apply directly for the description of isotropic compression of granular materials. While at a given pressure the contact theory would predict a relative change in volume

$$\frac{\Delta V}{V} = -3\varepsilon \tag{17}$$

the measured values deviate essentially from this ideal model in the sense that the tested samples become stiffer more rapidly than the model predictions.

For the further discussion all geometrical dimensions are normalized by the radius of the spheres, in a first approximation assumed to be equal for all particles. In the formula displayed above $\Delta V/V$ represents a relative change in volume V, e.g. represented by a cube L^3 as shown in figure 5. The change in half distance of the spheres centers varies according to

$$\varepsilon = p^{2/3} \tag{18}$$

where p is the "*hydrostatic*" pressure scaled by $p_0 = \frac{1}{3}\frac{E}{1-\nu^2}$ and ε denotes compressive strain. This scale is motivated by the Hertzian contact theory. Note, during isotropic compression the stress tensor reduces to $\boldsymbol{\sigma} = p\mathbf{I}$.

The formulas displayed above lead directly to the pressure-strain relation

$$p = \varepsilon^{3/2}. \tag{19}$$

Isotropic compression is difficult to realize experimentally. More popular are Oedometer measurements. In the later type of experiments a change in the bed height $\Delta H/H$ determines directly the relative change in volume. As a direct consequence of the equations (5) subject to the constraints $e_{11} = \Delta V/V = -3\varepsilon$, $e_{22} = e_{33} = 0$ it follows that $\sigma_{22} = \sigma_{33} = \frac{\nu^*}{1-\nu^*}\sigma_{11}$ and one finds finally that equation (19) still applies. During oedometric compression of granular materials values of $\sigma_{22} = \sigma_{33} = (0.4 \div 0.5)\,\sigma_{11}$ are often found which correspond to granular Poisson's ratios in the range of $\nu^* = 0.28 \div 0.33$.

If desired one can define a nondimensional effective bulk modulus as

$$k = \frac{dp}{d\varepsilon} = \frac{3}{2}\varepsilon^{1/2} = \frac{3}{2}p^{1/3}, \tag{20}$$

where $k = 3K^*/p_0$. Here, K^* stands for the granular bulk modulus of the whole packing. The condition displayed above holds for isotropic or nearly isotropic conditions, when $p \gg q$. If this condition is not satisfied one can derive relations that take into account small corrections for k due to deviatoric stress at order $O\left(q^2/p^2\right)$ (see Dubujet, Cambou, Dedecker and Emeriault (1997)).

In experiments, however, relations different from these are more likely found, which make the application to granular materials of the Hertz theory questionable and demands for modifications. As already shown for the 2D case of compressed cylinders the distribution in radii which has been neglected in a first model can be responsible for the behavior observed in compression experiments. The model reported by Ko and Scott (1967) seems to be a suitable tool for a description of the granular behavior in isotropic compression. From a physical point of view there should be no big difference between the model proposed by Ko and Scott (1967) and that presented by Endres (1990). While Endres (1990) presents a detailed statistical analysis Ko and Scott (1967) assume two types of regular assemblies, the simple cubic and the face centered cubic arrangement, which compose a real granular packing in fractions determined by the measured porosity.

Imagine an assembly of spheres of two different radii, which for regular cubic lattice is shown in figure 6. The radii differ only slightly so that their difference does not change the structure of the grid or accounts for the determination of void. However, during the first stage of compression only the larger spheres are in Hertzian contact. A threshold of load is required until the smaller spheres reach contact. Increasing the load further, the smaller spheres transmit additional forces between themselves and towards the larger ones, thus increasing the stiffness of the packing. It is assumed that contacts remain at the same places during compression, i.e. sliding is prohibited.

Ko and Scott (1967) assume that the randomly packed bed of spherical particles is formed by clusters of face centered cubic (FCC) and simple cubic (SC) arrangements, with porosity $n_{FCC} = 0.260$ and $n_{SC} = 0.476$, respectively. In experiments the porosity observed, n_{obs}, of real beds lies between these two ideal limits of the densest and the least dense packing.

$$n_{obs} = x n_{FCC} + (1 - x)\, n_{SC}, \tag{21}$$

where x is the fraction of face centered cubic grains. In the experiments described in Reimann, Müller, Arbogast and Thun (1997b) a porosity $n_{obs} = 0.38$, was measured which leads to $x = 0.63$. Since the Hertzian theory of contact applies for both types of ideal packings, results can be obtained separately for FCC and SC and combined

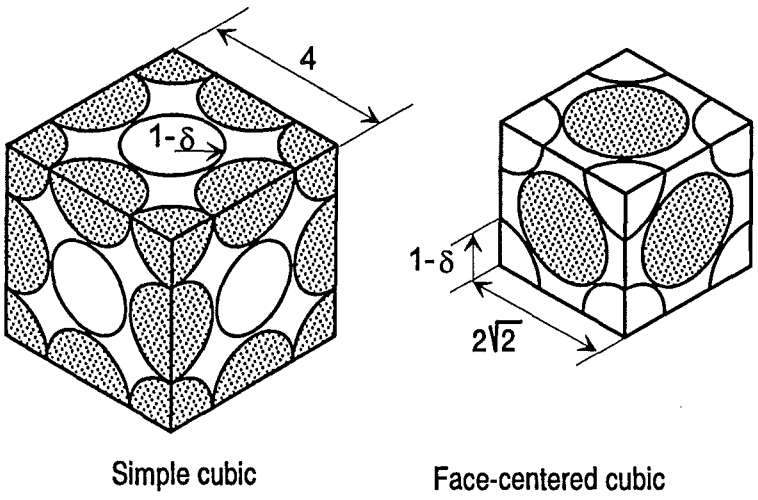

Figure 6: "Holey" unit elements of regular packings (see Ko and Scott (1967))

according their relative occurrence as determined by equation (21). As an example the ideas of the so-called "*Holey Model*" of Ko and Scott (1967) will be outlined for the *SC*-case. The basic ideas are as in the reference, but the analysis here differs in essential points. While in the paper by Ko and Scott (1967) the gaps close at distinct pressure, the present analysis assumes that gaps close at distinct strain. This should not make any difference in the physical behavior, but will reduce the determination of stress strain relation to simple integrals.

It is assumed in a first step that a typical volume element is formed by spheres of two radii, $r_1 = 1$ and $r_2 = 1 - \delta$. The symmetry of the volume element is a necessary condition since after isotropic compression all elements must still fit perfectly together to form the large body of granular material. Initially only the larger spheres with larger neighbors are in contact, leading to a pressure strain relation

$$p = \frac{1}{4}\varepsilon^{3/2} \quad \text{for } \varepsilon < \frac{1}{2}\delta. \tag{22}$$

After deformations large enough, $\varepsilon \geqq \frac{1}{2}\delta$, the gaps between the spheres close and the pressure is governed by the equation

$$p = \frac{1}{4}\varepsilon^{3/2} + \frac{3}{4}\left(\varepsilon - \frac{1}{2}\delta\right)^{3/2} \quad \text{for } \varepsilon \geqq \frac{1}{2}\delta. \tag{23}$$

The bulk elastic modulus thus becomes

$$k = \frac{dp}{d\varepsilon} = \begin{cases} \frac{3}{8}\sqrt{\varepsilon} & \varepsilon < \frac{1}{2}\delta \\ \frac{3}{8}\sqrt{\varepsilon} + \frac{9}{8}\sqrt{\varepsilon - \frac{1}{2}\delta} & \varepsilon \geqq \frac{1}{2}\delta \end{cases} \quad \text{for } SC. \tag{24}$$

This result is sketched in figure 7. First the sample becomes stiffer according to the Hertz theory, but with a reduced number of contacts. As $\varepsilon \geqq \frac{1}{2}\delta$ all gaps are closed with the result that the stiffness increases more rapidly.

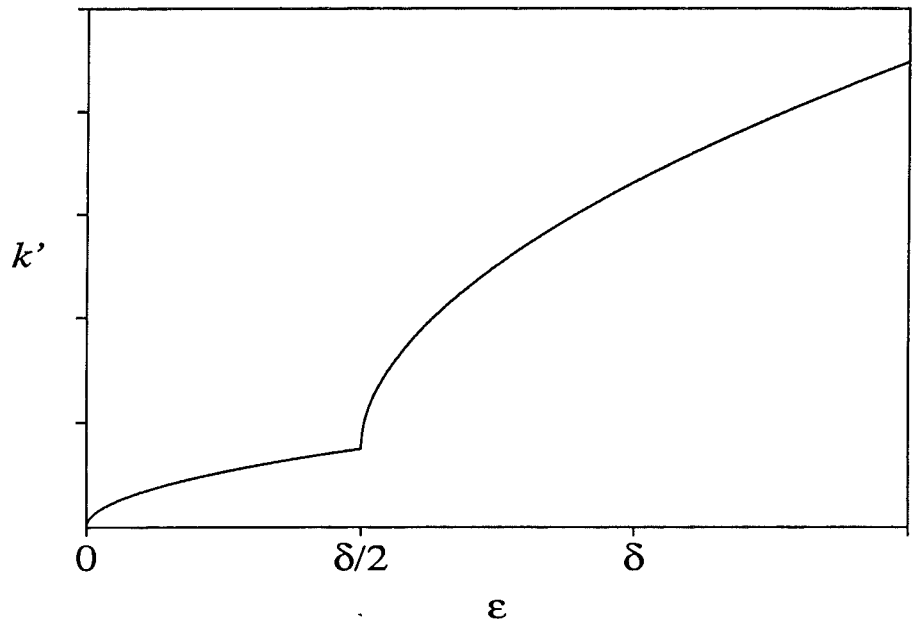

Figure 7: Elastic modulus for the "Holey" simple cubic arrangement versus ε. The characteristic dependency changes when the gaps close at $\varepsilon = \frac{1}{2}\delta$.

In real granular beds there are not only spheres with two distinct radii. Instead, the particles will exhibit a continuous distribution in size. It is assumed now that the radius of the largest particle is $r = 1$ and that the gaps are distributed according to a truncated Gaussian $G(d = \delta/\delta_0)$ as shown in figure 8.

$$G \sim \exp\left[-\frac{1}{2}\left(\frac{d-1}{s}\right)^2\right] - \exp\left[-\frac{1}{2}\left(\frac{1}{s}\right)^2\right] \quad \text{for } 0 < d < 2. \tag{25}$$

The amplitude is chosen such that the integral from 0 to 2 becomes unity.

For the further analysis it is suitable to rascal the problem with δ_0, the most probable gap size. With the substitution of the variables $k = k' \cdot \sqrt{\delta_0/2}$, $\varepsilon = e \cdot \delta_0/2$ and $\delta = d \cdot \delta_0$ the rescaled bulk elastic modulus becomes

$$k'(e,d) = \begin{cases} \frac{3}{8}\sqrt{e} & e < d \\ \frac{3}{8}\sqrt{e} + \frac{9}{8}\sqrt{e-d} & e \geqq d \end{cases} \quad \text{for } SC. \tag{26}$$

The elastic modulus of the whole assembly is obtained via the differential summation of reciprocal values as

$$\frac{1}{k'(e)} = \int_0^2 \frac{G(d)}{k'(e,d)} d(d). \tag{27}$$

The results for $k'(e)$ are plotted in figure 9. For small deformations the Elastic modulus is obtained by Hertzian contact between a reduced number of spheres while for large deformations the sample behaves as if all spheres are in contact. For small and large deformations the elastic modulus behaves similar as for the case with a single gap size,

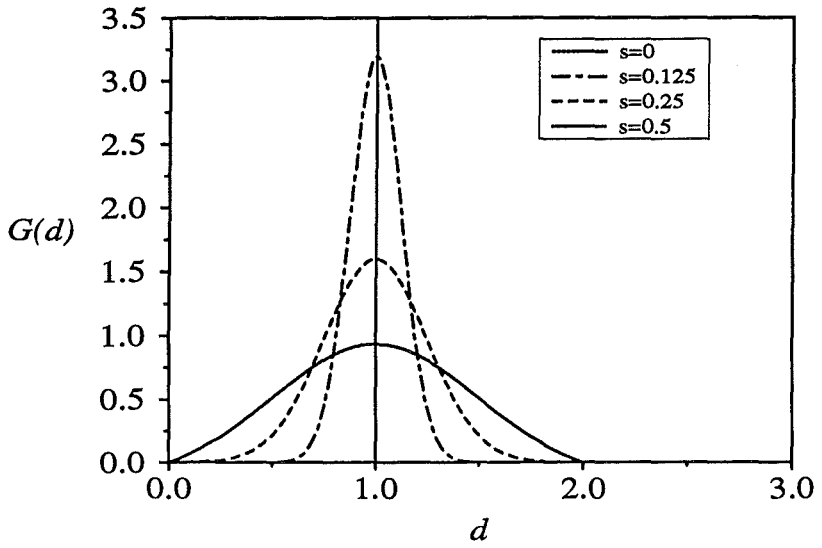

Figure 8: Distribution of gap size between two spheres in the "holey" model. The Gaussian has been truncated since negative values of $d = \delta/\delta_0$ do not occur. The most probable gap size is δ_0.

i.e. $s = 0$ as sketched in the same figure for comparison. For packings with distributed gap size the curves become smoothed and now deviate essentially from the square root law of the pure Hertzian theory in the range of gap size between $0 \lesssim d. \lesssim 2$.

Recently, Reimann et al. (1997b) published experimental results for the compression of spheres made of glass and orthosilicate. After consolidation they find the results shown in figure 11. They focus their presentation on the quantity $K/\sqrt{p}$. Since they plot their results versus pressure a direct comparison requires that also the pressure is calculated from the present theory. This is done as

$$p'(e) = \int_0^e k'(e)\, de. \tag{28}$$

The bulk elastic modulus k' rescaled with pressure as $k'/\sqrt{p'}$ is plotted versus p' in figure 12. The present theory never suggests such a scale. The plot has been shown here with the only intention to have a comparison with results published by Reimann et al. (1997b). The qualitative agreement with the experimental observations is relatively good. The theory predicts a decrease of $k'/\sqrt{p'}$ with larger values of pressure as it is found in the experiments. Approaching lower pressure values $k'/\sqrt{p'}$ first decrease and later increase strongly as $p' \to 0$. Similar effects have been found in the experiment cited, most pronounced for beds of orthosilicate. It should be possible to find a distribution of gap size say a value of s that fits best the measured data. One should note, however, that the increase for small p of the quantity $k/\sqrt{p}$ has not been observed in proceeding experiments (Reimann, private communication) so that the behavior in this range of

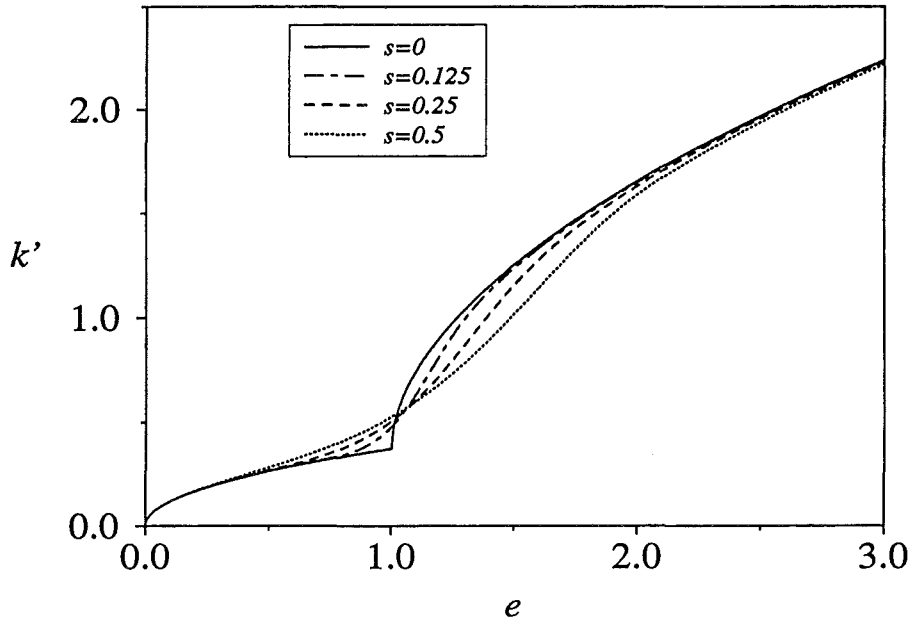

Figure 9: Bulk elastic modulus k' versus e for several gap size distributions according to the assumed Gaussians

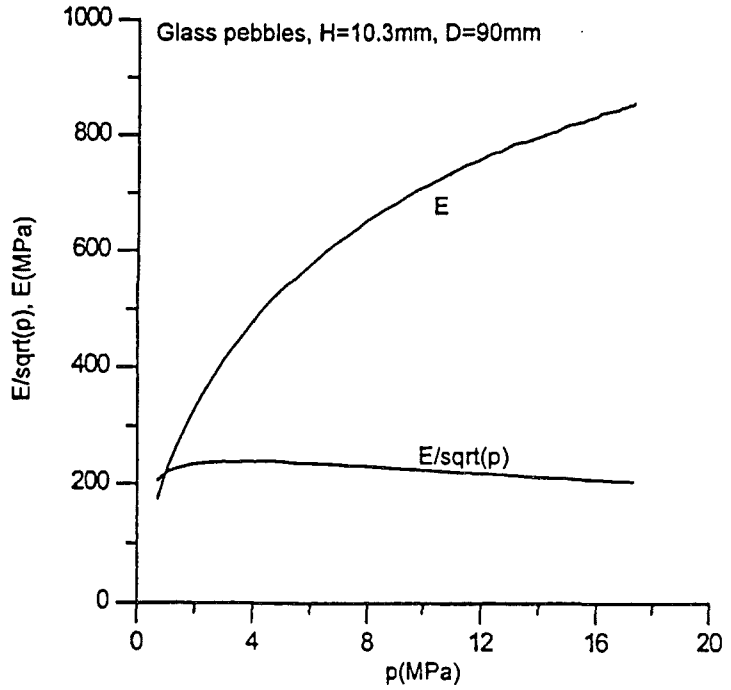

Figure 10: compression of glas spheres. Results obtained by Reimann et al. (1997b). Results are scaled by these authors and presented as $K/\sqrt{p}$ versus p. The dimensions of the apparatus are $H = 10.3mm$, $D = 90mm$.

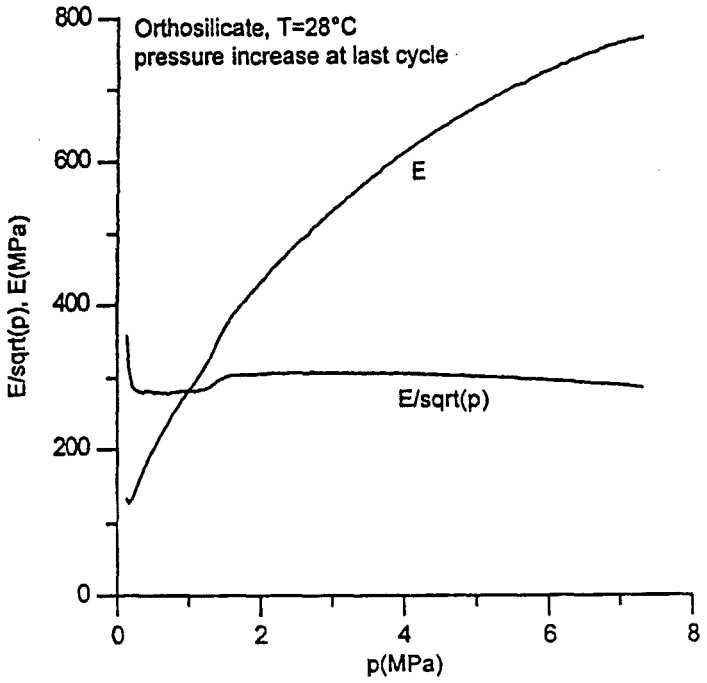

Figure 11: compression of orthosilicate spheres. Results obtained by Reimann et al. (1997b). Results are scaled by these authors and presented as $K/\sqrt{p}$ versus p. The dimensions of the apparatus are $H = 12mm$, $D = 60mm$. Similar results have been observed by Duchesne and Raepsaet (1996) (p 22/33)

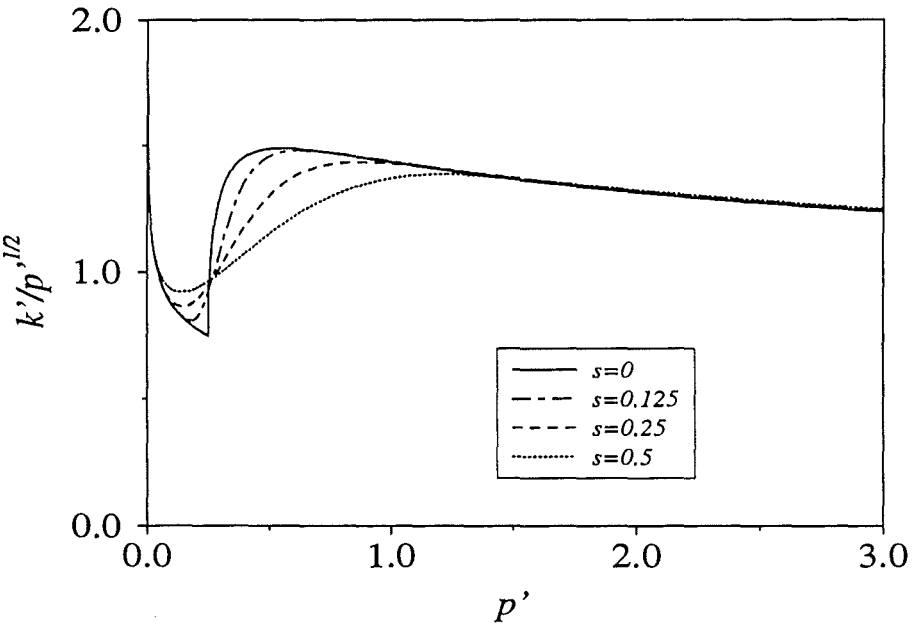

Figure 12: Calculated rescaled bulk elastic modulus rescaled with pressure as $k'/\sqrt{p'}$ as a function of pressure p' for the granular assembly with distributed gap size.

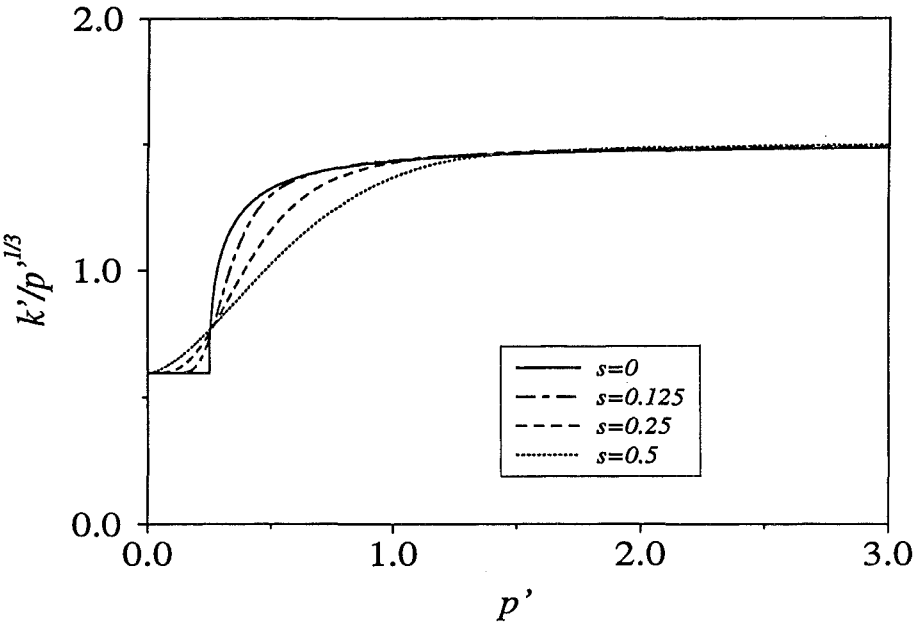

Figure 13: Calculated bulk elastic modulus properly rescaled with pressure as $k'/p'^{1/3}$ as a function of pressure p' for the granular assembly with distributed gap size.

parameter is probably hard to resolve experimentally (very small deformations and pressures).

If the results for the elastic modulus are scaled, as the theory suggests, with $p'^{1/3}$ instead of $\sqrt{p'}$ one can see more clearly the physical phenomena (see figure 13). For small compression only the larger spheres are in contact. This leads to results according to the Hertz theory where $k' \sim p'^{1/3}$. As $p' \to 0$, $k'/\ p'^{1/3}$ approaches the value of $\frac{3}{8}2^{2/3}$. For large compression all gaps are closed so that the Hertzian theory applies for all connections between spheres with again, $k' \sim p'^{1/3}$ for $p' \gtrsim 1.5$. As $p' \gg 1$ the quantity $k'/p'^{1/3}$ becomes close to 3/2. One has to expect that a representation of the results obtained by Reimann et al. (1997b) using this scale should confirm these effects.

At this place it should be kept in mind that the analysis above has been performed for the simple cubic arrangement of the spheres. In real beds volume fractions x with FCC and $(1-x)$ with SC are present simultaneously. For FCC the elastic behavior is quite similar as for SC and characterized by the following equation:

$$k'(e,d) = \begin{cases} \frac{3}{\sqrt{2}}\sqrt{e} & e < d \\ \frac{3}{\sqrt{2}}\left(\sqrt{e}+\sqrt{e-d}\right) & e \geqq d \end{cases} \quad \text{for } FCC. \tag{29}$$

For a specific value of x one can now calculate the elastic modulus according to the weights of FCC and SC. Results are displayed in figure 14 for $s = 0.1$. The scales are chosen to allow a comparison with results obtained by Reimann et al. (1997b). The thick curves correspond to limiting values of x namely $x = 0$ (SC) and $x = 1$ (FCC). The elastic modulus of any real assembly of grains must lie between these two curves.

Better insight into the physics may be gained by the same data plotted now as k' versus p' in a log-log plot (see figure 15). One finds the slope equal to 1/3 according

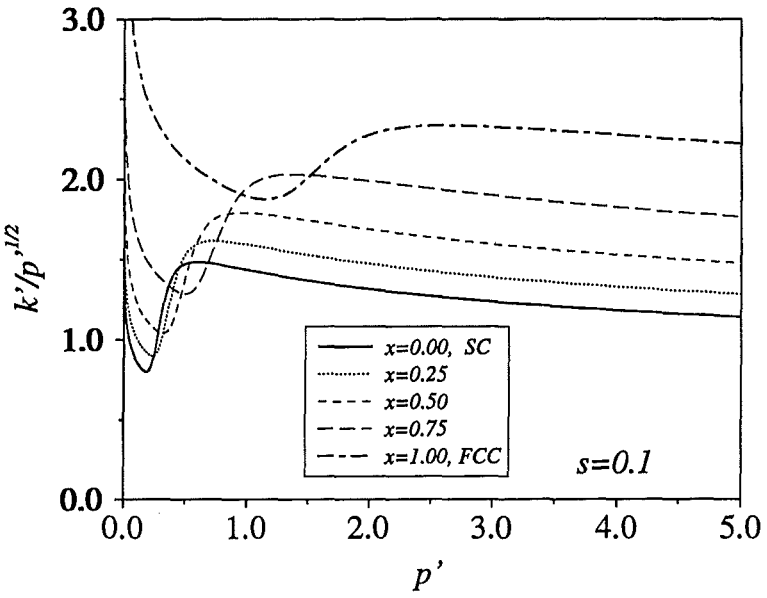

Figure 14: $k'/\sqrt{p'}$ as a function of p'. Results are shown for different values of the packing density, characterized by the parameter x. The values $x = 0$ and $x = 1$ correspond to the least dense and the most dense regular arrangement, the simple cubic SC and the face centered cubic FCC assemblies, respectively.

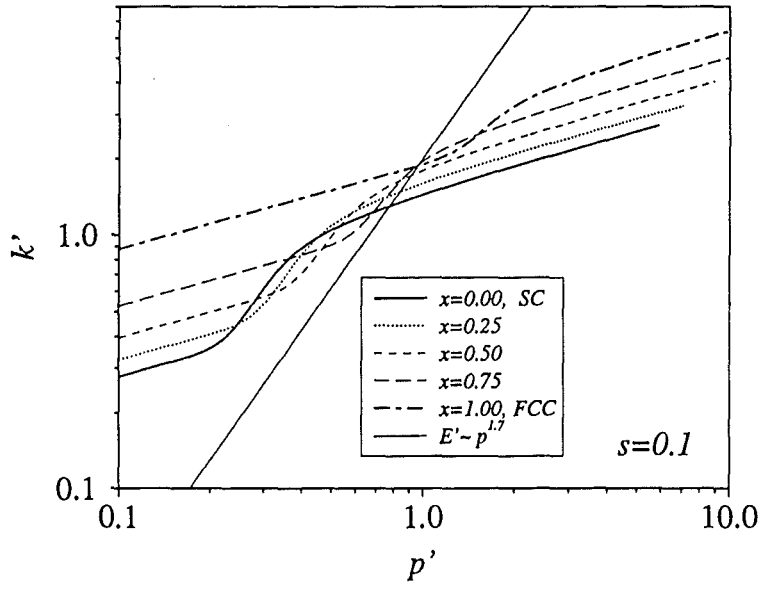

Figure 15: k' as a function of p' (same data as in previous figure). This graph shows most clearly the physical relations. Results are shown for different values of the packing density, characterized by the parameter x. The values $x = 0$ and $x = 1$ correspond to the least dense and the most dense regular arrangement, the simple cubic SC and the face centered cubic FCC assemblies, respectively.

to the Hertz theory for very small and very large p'. In an intermediate region one can identify a slope of 1.7 that corresponds to the exponent $m = 2.7$ according to equation (13), often found in experiments. It is possible that the lower Hertzian range can not be observed in experiments because the values of pressure are not resolved by the measuring techniques. In that case the measurements start with the intermediate range in qualitative accordance to the predictions. It should be noted that the slope in the intermediate range depends essentially on the distribution of the gap size. A narrower distribution gives a larger slope. This may explain the wide range ($2,7 < m < 3.5$, Guyon et al. (1990)) observed experimentally by the fact that different materials differ in this property.

Most reports of Reimann & co-authors and also other publications show not only the derived quantities like the elastic modulus but also the basic data measured, the stress or more precisely $p = -\frac{1}{3}\sigma_{kk}$ versus the deformation $-\Delta V/V$. For a comparison with these results the same presentation is used in figure 16. In the figure some of the last cycles published in Reimann and Müller (1998) are shown together with the theoretical prediction. The parameters used in the model are also given in the figure. The stress σ_{11} is applied and measured while the stresses $\sigma_{22} = \sigma_{33}$ are estimated as $0.4\sigma_{11}$ according to experimental experience (Herle, UNI Karlsruhe, personal communication), a value that corresponds to a granular Poisson ratio of $\nu^* = 0.28$.

Note, in uniaxial compression tests the ratio $(q/p)^2$ may approach unity so that a more accurate approximation of the bulk elastic modulus would require a correction by terms on the order of $(q/p)^2$. Dubujet et al. (1997), however, showed that such corrections are still small and do not contribute more than a few percent. These corrections would be much smaller than the effects caused by the gap closing model and are therefore neglected here.

Of course, a simple elastic model is unable to predict the hysteresis observed during the experiment. At low deformations, the stresses during the loading period are higher in the experiment than predicted. This should have its explanation in the fact that during this stage the gaps have to close. Particles will exert Coulomb friction during microscopic movements. Thus, more energy is required to get a specific deformation than is stored within the elastic body. Once most gaps are closed, the deformation is mainly elastic and follows the predictions. During the unloading cycle the friction is active until most gaps are opened. From that point on, the packing behaves like an elastic one approaching the theoretical predictions again. From this comparison one can conclude that the model reproduces the experimental data with sufficient accuracy in order to predict stresses for engineering applications (but not for the first pressure increase).

Finally one can conclude that the Holey Model is a suitable tool for interpreting the experimental observation of Reimann and Müller (1998). Results deviate essentially from the classical Hertzian theory of contact for deformations on the order of the gap size between particles. For smaller deformations the Hertzian theory still applies but with a reduced number of contacts leading to relatively weak assemblies. For much larger deformations the packed bed behaves as a dense ideal packing according to the contact theory supposed that internal stresses do not exceed the value at which particles crack. The model contains the parameters δ_0 and s. If these are unknown one can adjust the

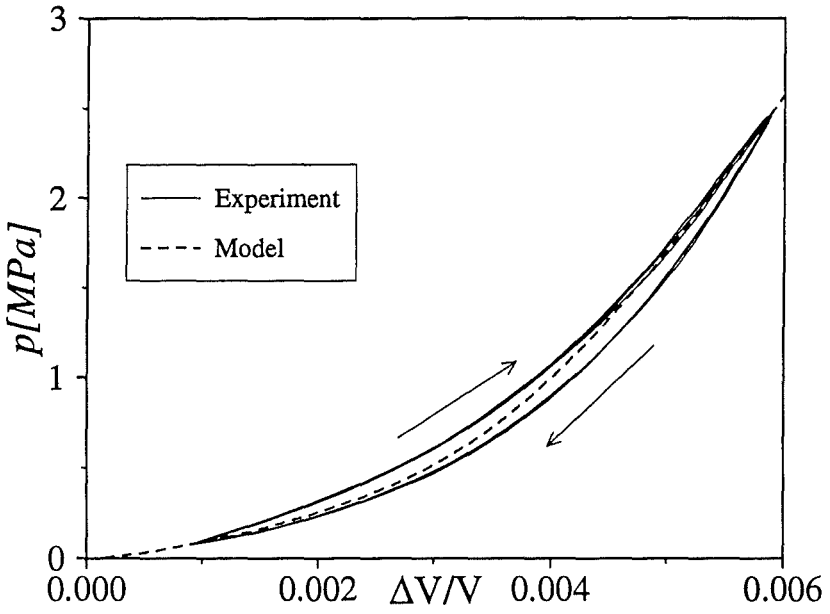

Figure 16: p versus $-\Delta V/V$ for comparison with basic data from experiments e.g. Reimann and Müller (1998). The experimental curve is taken after intense mechanical cycling (about 2000 cycles), i.e. when the bed approaches final density. The theoretical results have been calculated using the parameters $\delta_0/2 = 0.9 \cdot 10^{-3}$, $s = 0.25$, $E = 0.103 \cdot 10^6 MPa$, $\nu = 0.25$ (Zimmermann (1989) eq. 4) and a porosity of $n_{obs} = 0.38$.

two parameters -the most probable gap size δ_0 and the distribution parameter s for a best fit with the experimental data.

4 Wall friction in uniaxial compression

During Oedometer experiments one observes usually a hysteresis in a pressure strain diagram (see e.g. figure 16). Moreover, the first pressure increase differs essentially from the subsequent ones. It will be shown in the following subsection that these effects can, at least partly, be caused by wall friction in the uniaxial test apparatus. The following analysis oversimplifies the real stress state by considering only the spherical part of the stress tensor. It is not intended to give precise data but to shed some light on the physical mechanisms involved using a mathematical representation as simple as possible.

Consider a cylindrical uniaxial test facility with radius r and length (height) l. Let the axial coordinate x start at the position where the force $2\pi r\sigma_x$ is introduced by a movable wall. The quantity σ_x denotes the normal stress in axial direction. The radial stresses are related to the axial one as $\sigma_r = \frac{\nu^*}{1-\nu^*}\sigma_x$. A force balance at the differential element $2\pi r dx$ leads to the differential equation governing the axial stress

$$\partial_x \sigma_x \pm \sigma_x = 0 \tag{30}$$

when the weight of the pebbles is negligible in comparison with the applied forces. The coordinate x (as well as the length l used later) is scaled by $r\left(f\frac{\nu^*}{1-\nu^*}\right)^{-1}$, where f is the coefficient of wall friction. The solution is simply an exponential

$$\sigma_z = \sigma_\pm e^{\mp x}. \tag{31}$$

The signs $+$ and $-$ stand for compression and relaxation, respectively. The spherical part of stress is obtained as

$$p = \frac{1}{3}\left(\frac{1+\nu^*}{1-\nu^*}\right)\sigma_\pm e^{\mp x} = p_\pm e^{\mp x}. \tag{32}$$

If a pressure p_+ is applied at $x = 0$ during compression the transmission into the bed is described by the above exponential. This relation is generally known and has been already presented in a paper by Dantu (1967). Such a state of stress is related to local strain via the elasticity of the bed

$$e_x = 3\varepsilon \quad \text{with } \varepsilon = \varepsilon(p) \tag{33}$$

as derived in previous subsections. The total deformation Δl becomes therefore

$$\Delta l = \int_0^l 3\varepsilon(p)\, dx. \tag{34}$$

As the simplest example, consider for a moment the case of a regular packing of spheres with uniform size for which the Hertz contact theory leads to

$$\varepsilon = p^{2/3}. \tag{35}$$

More detailed analyses using gap closing models are possible, but these would require numerical methods of solution and do not contribute much for physical understanding.

With these assumptions one can estimate the deformation during the compression phase as

$$\Delta l = 3 \int_0^l \left(p_+ \mathrm{e}^{-x}\right)^{2/3} dx = \frac{9}{2} p_+^{2/3} \left(1 - \mathrm{e}^{-2l/3}\right). \tag{36}$$

The most interesting result is that for infinitely thick beds, $l \to \infty$, the change in length asymptotes to a value independent of the bed height. The reason is that the walls carry a fraction of the induced load so that in some depth only a negligible part remains inside the packing. If now someone would estimate the pressure increase as a function of $\Delta l/l$ the stiffness of the whole assembly would be overestimated, especially for beds with a large aspect ratio, $l \gg 1$. In any case it would be better to use flat beds in order to minimize wall friction. In the experiments used for a comparison with the present elastic analysis Reimann and Müller (1998) used relatively flat beds with a height to radius ratio of 0.46. For small values of l the ratio $\Delta l/l$ asymptotes towards a unique value and almost the whole assembly of granular material will exert the same state of compression. For $l \to 0$ the hysteresis due to wall friction will become negligible. A remaining hysteresis is then caused by internal friction of the granular material.

This simple consideration already demonstrates that it is hard to transmit forces along confined granular packings over nondimensional distances larger than $O(1)$. Only a first part of a long bed would be affected by compression if the stress were applied at one end.

Imagine now a situation when a maximum pressure $p_{+,1}$ has been applied during a first compression cycle. The situation is sketched in figure 17. This leads to a deformation $\Delta l_{+,1}$. During a proceeding relaxation step the pressure p_- decreases from $p_{+,1}$ monotonically to a value $p_{-,1}$, the minimum value after the first cycle. It is obvious, that the fraction of the test sample is unloaded in which the pressure p_- is lower than the previously applied pressure p_+. In the unloaded part $0 < x < l_-$ the pressure varies according to

$$p = p_- \mathrm{e}^x \quad \text{for } 0 < x < l_-, \tag{37}$$

whereas the rest of the sample keeps its compressed state according to

$$p = p_{+,1} \mathrm{e}^{-x} \quad \text{for } l_- < x < l. \tag{38}$$

Both conditions determine the coordinate $x = l_-$ which separates the compression and relaxation domains or in other words the passive and active regions of the granular bed. Of course, l_- can not exceed the value l so that finally

$$l_- = \min\left(\frac{1}{2} \ln \frac{p_{+,1}}{p_-},\ l\right). \tag{39}$$

The total deformation $\Delta l\,(p_-)$ of the bed then becomes

$$\Delta l = 3 \left[\int_0^{l_-} \varepsilon\left(p_- \mathrm{e}^x\right) dx + \int_{l_-}^{l} \varepsilon\left(p_{+,1} \mathrm{e}^{-x}\right) dx\right]. \tag{40}$$

During a proceeding loading the applied pressure p_+ may increase again from $p_{-,1}$ and create inside the test sample a distribution according to the equation (32). The total

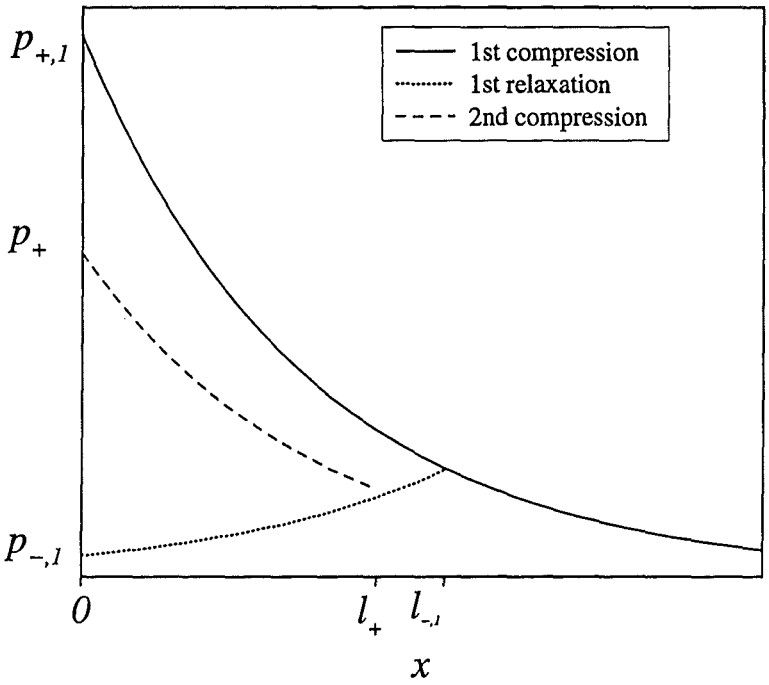

Figure 17: Pressure distribution in a uniaxially compressed sample with wall friction. In a first compression the pressure at $x = 0$ is increased up to $p_{+,1}$. In a first relaxation the pressure decreases to $p_{-,1}$. During the second compression the pressure p_+ increases again.

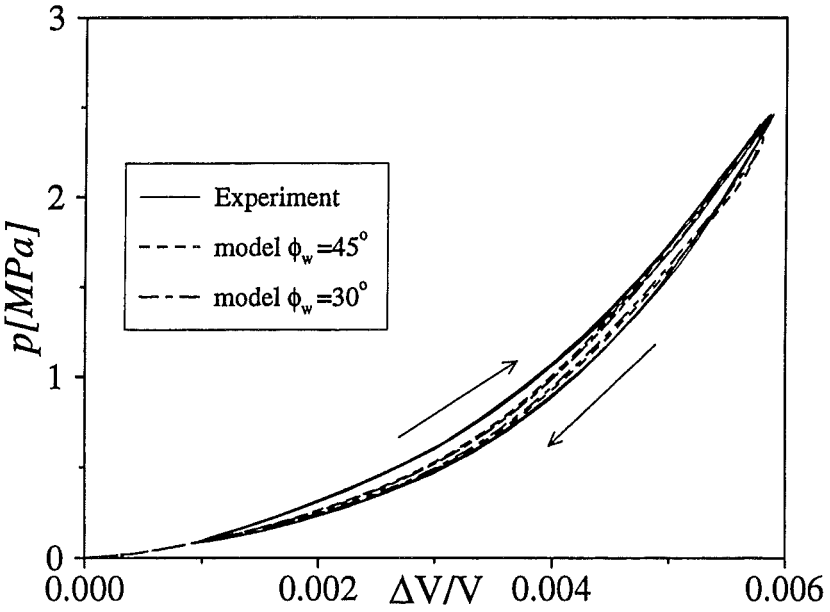

Figure 18: Comparison of experimental results (Reimann and Müller (1998)) with theoretical data using an elastic model and wall friction. For negligible wall friction the hysteresis disappears in the analysis.

deformation during the second compression is now obtained by

$$\Delta l = 3\left[\int_0^{l_+} \varepsilon\left(p_+ \mathrm{e}^{-x}\right) dx + \int_{l_+}^{l_{-,1}} \varepsilon\left(p_- \mathrm{e}^{x}\right) dx + \int_{l_{-,1}}^{l} \varepsilon\left(p_{+,1} \mathrm{e}^{-x}\right) dx\right], \tag{41}$$

where l_+ characterizes the length of the sample which is affected by the new compression.

$$l_+ = \min\left(\frac{1}{2}\ln\frac{p_+}{p_{-,1}}, l_{-,1}\right) \tag{42}$$

The variable $l_{-,1}$ characterizes the value of l_- at the end of the first stress relaxation. Since this is only a part of the total length, the sample behaves stiffer than during the first cycle up to the point when the applied pressure exceeds the maximum value $p_{+,1}$ applied during the preceding loading.

The evaluation of the formula displayed above results in the data shown in figure 18. One observes a hysteresis, the width of which becomes smaller with smaller wall friction.

The value of $f\frac{\nu^*}{1-\nu^*}$ has been estimated for experiments using Li_2ZrO_3 pebbles to give 0.399 Ying and Abdou (1998). This would correspond to a value for skin friction of about $f \sim 1$ or a wall friction angle of $\phi_w = 45°$. There is no such data available for Li_2SiO_4. Comparing the results displayed in figure 18 one can argue that similar values should hold for Li_2SiO_4 as well.

The present model has been applied to the geometry (height to radius ratio about 4.8) as used for the uniaxial compression tests by Ying and Abdou (1998). Results are

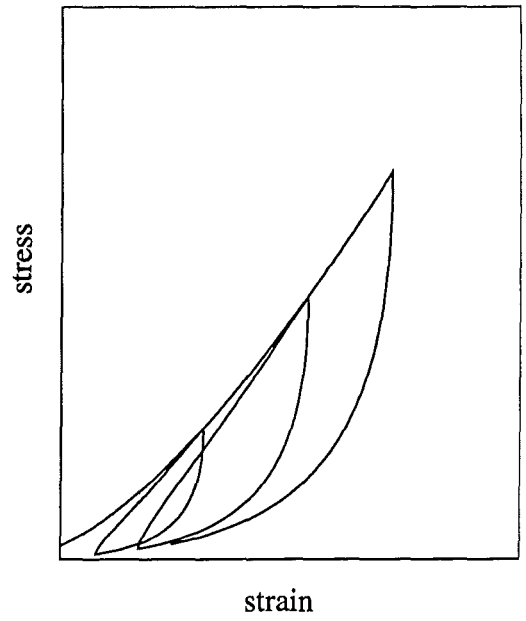

Figure 19: Calculated stress strain relation for three loading-relaxation cycles in a uniaxial compression facility with geometry similar to that used by Ying and Abdou (1998). A quantitative comparison was impossible because a lack of material data.

shown in the figure 19. The qualitative agreement with experimental results shown in figure 20 supports again the ideas outlined above that significant part of effects observed in such experiments can be related to elastic compression and wall friction. Moreover, it may be hard to distinguish between both effects. A quantitative comparison was not possible because not all material data was given in Ying and Abdou (1998).

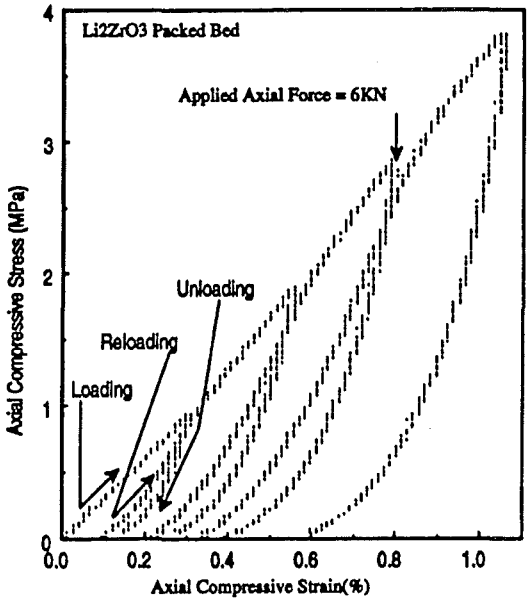

Figure 20: Experimental data for several compression-relaxation cycles (figure taken from Ying and Abdou (1998)) The height to radius ratio was about 4.8.

5 Conclusions

The bulk elastic behavior of an assembly of elastic particles (spheres) has been analyzed using the so-called *"Holey"* model proposed by Ko and Scott (1967), which is quite analog to the *contact generation* model used by Endres (1990). It is assumed that a real dense packing is built up by regions occupied by simple and face centered regular cubic assemblies. It is further assumed that the spheres have slightly different radii so that gaps are possible which reduce the number of particles in contact. During loading gaps are closed successively, a fact that increases the stiffness of the bed faster than predictions according to the classical Hertz theory of contact. After all gaps are closed a further compaction will lead to a stiffness approaching expectations according to the contact theory. In an intermediate region the results deviate essentially from the Hertz predictions. The difference in radii between spheres has been assumed to be small. This is not really a necessary assumption since the comparison with experimental data shows a good agreement even if the radii of the spheres vary within a range $0.2mm$ to $0.6mm$.

The model has been applied to the packed bed of Li_2SiO_4 pebbles and compared with experimental results. Within the range of measured data the model gives a good approximation of the physics after a number of loading cycles. The model can not be used to describe the first compression since the bed must find the most dense packing before the theory applies. A description of the first pressure increase with the present model fails because important features in this process are not jet included in the model. One can imagine that this may be possible by modelling internal friction or instabilities in loaded bridges.

Finally an attempt was made to explain hysteresis effects between loading and relaxation cycles. Using reasonable arguments one can derive a simple model which takes into account the friction between the granular bed and the confining walls for uniaxial compression tests. The model predicts a hysteresis, the width of which becomes larger with the axial length of the bed. For flat samples the hysteresis due to wall friction may become very weak. In the latter case the remaining hysteresis should be related to internal friction which is not jet included in this simple model. If the height of the bed reaches order unity, wall friction becomes the dominant effect and one should be careful with the interpretation of elastic results obtained by such experiments. The analysis shows further that it is impossible to transmit forces in a bed confined by parallel plates over distances much larger than the plate distance.

References

Dalle Donne, M., Fischer, U., Norajitra, P., Reimann, G. and Reiser, H.: 1995, European DEMO BOT solid breeder blanket: The concept based on the use of cooling plates and beds of berylium and Li_4SiO_4 pebbles, *in* K. Herschbach, W. Maurer and J. E. Vetter (eds), *Fusion Technology 1994*, Vol. 2, Elsevier, pp. 1157–1160.

Dantu, P.: 1967, Étude expérimentale d'un milieau pulvérulent. Compris entre deux plans verticaux et parallèles, *Annales des Ponts et Chaussées* **IV**, 193–202.

Dubujet, P., Cambou, B., Dedecker, F. and Emeriault, F.: 1997, Statistical homogenization for granular media - Application to non linear elastic medelling, *in* Behringer and Jenkins (eds), *Powders & Grains 97*, Balkema, pp. 1–13.

Duchesne, A. and Raepsaet, X.: 1996, Compte rendu de la champagne d' essais triaxiaux sur matériaux granulaires à grains arrondis, *Technical Report DMT 96/353, SERMA/LCA/1929*, CEA.

Durelli, A. J., Phillips, E. A. and Tsao, C. H.: 1958, *Introduction to the Theoretical and Experimental Analysis of Stress and Strain*, McGraw-Hill Series in Mechanical Engineering, McGraw-Hill Book Company, INC.

Endres, A. L.: 1990, The effect of contact generation on the elastic properties of a granular medium, *Transactions of the ASME* **57**, 330–336.

Guyon, E., Roux, S., Hansen, A., Bideau, D., Troadec, J.-P. and Crapo, H.: 1990, Non-local and non-linear problems in the mechanics of disordered systems: applications to granular media and rigidity problems, *Reports on Progress in Physics* **53**, 373–419.

Hunter, S. C.: 1983, *Mechanics of continuous media*, Ellis Horwood Series in Mathematics and its Applications, 2nd edn, Ellis Horwood Limited.

Ko, H.-Y. and Scott, R. F.: 1967, Deformation of sand in hydrostatic compression, *Journal of the Soil Mechanics and Foundation Division, Proceeding of the American Society of Civil Engineers* **SM3**, 137–156.

Reimann, J. and Müller, S.: 1998, Thermomechanical behaviour of Li_4SiO_4 pebble beds., *Fusion Technology 1998, Proceedings of the 20th Symposium on Fusion Technology, Marseilles, September 7-11, 1998.*

Reimann, J., Müller, S. and Lenartz, M.: 1997a, *Technical Report Unveröffentlichter Bericht*, Forschungszentrum Karlsruhe.

Reimann, J., Müller, S., Arbogast, E. and Thun, G.: 1997b, *Technical Report Unveröffentlichter Bericht*, Forschungszentrum Karlsruhe.

Stauffer, D., Herrmann, H. J. and Roux, S.: 1987, Simulation of disordered systems of cylinders: II Mechanical behavior, *Journal de Physique* **48**, 347–351. Z4-04.

Walton, K.: 1987, The effective elastic moduli of a random packing of spheres, *J. Mech. Phys. Solids* **35**(2), 213–226.

Ying, A. Y. and Abdou, M. A.: 1998, Analysis of thermomechanical interactions and properties of ceramic breeder blankets, *Fusion Engineering and Design.* Presented at the ISFNT-4, Tokyo, April 7-11, 1997.

Zimmermann, H.: 1989, Mechanische Eigenschaften von Lithiumsilikaten für Fusionsreaktor-Brutblankets, *Technical Report KfK 4528*, Kernforschungszentrum Karlsruhe.